

the velocity profiles considerably. In conclusion, it might be noted that Eq. (3) is a special case of a more general law for the outer region of equilibrium turbulent boundary layers.⁸

References

- ¹ Mickley, H. S. and Smith, K. A., "Velocity defect law for a transpired turbulent boundary layer," *AIAA J.* 1, 1685 (1963).
- ² Black, T. J. and Sarnecki, A. J., "The turbulent boundary layer with suction or injection," *Aeronautical Research Council of London Rept.* 20,501 (1958).
- ³ Stevenson, T. N., "A law of the wall for turbulent boundary layers with suction or injection," *College of Aeronautics, Rept.* 166 (1963).
- ⁴ Millikan, C. B., "A critical discussion of turbulent flows in channels and circular tubes," *Proceedings of the Fifth International Congress of Applied Mathematics* (John Wiley and Sons, Inc., New York, 1959), pp. 386-392.
- ⁵ Stevenson, T. N., "A modified velocity defect law for turbulent boundary layers with injection," *Aeronautical Research Council of London Rept.* 20, 501 (1958).
- ⁶ Mickley, H. S. and Davis, R. S., "Momentum transfer for flow over a flat plate with blowing," *NACA TN* 4017 (1957).
- ⁷ Dutton, R. A., "The effects of distributed suction on the development of turbulent boundary layers," *Aeronautical Research Council of London, R&M* 3155 (1960).
- ⁸ Stevenson, T. N., "A note on the outer region of turbulent boundary layers," *College of Aeronautics Note* (to be published).
- ⁹ Townsend, A. A., *The Structure of Turbulent Shear Flow* (Cambridge University Press, Cambridge, England, 1956), Chap. 10, p. 245.

Exact Two-Body Error Sensitivity Coefficients

K. C. KOCH†

North American Aviation, Inc., Anaheim, Calif.

Nomenclature

- r = radial distance to dynamical center
- p = semilatus rectum
- n^* = $(\mu/p^3)^{1/2}$ = modified mean motion parameter
- v = true anomaly
- e = eccentricity
- τ = $t - t_0$ = time since initial epoch
- Δx = inertial horizontal in-plane position deviation
- Δy = inertial out-of-plane position deviation
- Δz = inertial radial position deviation
- $\Delta \dot{x}^*$ = inertial horizontal in-plane velocity deviation
- $\Delta \dot{y}^*$ = inertial out-of-plane velocity deviation
- $\Delta \dot{z}^*$ = inertial radial velocity deviation
- μ = gravitational constant of primary body
- p/r = $1 + ecv$ = nondimensional
- cv, sv = $\cos v, \sin v$
- K_i = constants of integration $i = (1, 2, \dots, 6)$
- C_i = arbitrary constants
- W = $sv(1 + ecv)$ = integrating factor
- M_2 = $M_1 cv + M_1' sv + 2(r/p)M_2$

Introduction

TABLE 1 of Ref. 1 presented a complete set of exact first-order error sensitivity coefficients for the general Keplerian reference orbit. This note presents an outline of its derivation. As noted in Ref. 1, there are two ways of approaching this solution. One method involves perturbing the two-body integrals with respect to the orbit constants rela-

tive to the final and initial epochs.² These perturbations are combined by elimination to yield the error sensitivity coefficients or the transition matrix. The other approach that is considered herein is to integrate directly the perturbation equations of motion. This latter approach is more pertinent to guidance theory.

Prior to publication of Ref. 1, in the recent literature there did not appear to be an exact, completely explicit solution to this problem by either method for a general Keplerian orbit. Danby³ does give a complete solution by the former approach, but does not explicitly multiply out the 6×6 matrizants to yield the transition matrix. If he had multiplied the matrizants, the results of Table 1 of Ref. 1 would be obtained. Geyling⁴ develops the general linear perturbation equations, but he also gives the solution on the basis of the former approach, stating, however, that the two approaches are equivalent. He does not give a complete solution to this problem and specializes to $v_0 = 0$ for in-plane perturbations.

The primary objective here is to tie the complete set of exact error coefficients (Table 1 of Ref. 1) to the linear perturbation equations of motion by outlining its derivation. Thereby, valuable insights can be gained on the nature of error propagation in a free-fall trajectory, on the structure of mechanization ("patched conic") of the navigation-guidance problem and on analytic error propagation for the nonhomogeneous solution required for the guidance problem. (Note: The transition matrix is the Green's matrix for the nonhomogeneous problem.) Further details on this derivation can be found in Refs. 2 and 5.

Derivation of Error Coefficients

The error coefficients are obtained upon solving the following linear perturbation equations of motion as an initial value problem:

$$\Delta \ddot{\mathbf{r}} - 2\omega \Delta \dot{\mathbf{r}} + (-\omega + \omega^2) \Delta \mathbf{r} = -\frac{\mu}{r^3} \left[I - \frac{3\mathbf{r} \mathbf{r}^T}{r^2} \right] \Delta \mathbf{r} \quad (1)$$

where ω is the angular velocity matrix of the rotating frame. For a locally level in-plane out-of-plane coordinate system, one can write the components of $\Delta \mathbf{r}$

$$\Delta \mathbf{r} = \begin{bmatrix} \Delta x \\ \Delta y \\ \Delta z \end{bmatrix} = \begin{bmatrix} \text{inertial in-plane horizontal perturbation} \\ \text{inertial out-of-plane perturbation} \\ \text{inertial radial perturbation} \end{bmatrix} \quad (2)$$

and, if the reference trajectory is Keplerian, ω can be expressed as

$$\omega = \begin{bmatrix} 0 & 0 & -\dot{v} \\ 0 & 0 & 0 \\ \dot{v} & 0 & 0 \end{bmatrix}; \quad \dot{v} = \frac{(\mu p)^{1/2}}{r^2} \quad (3)$$

The associated inertial velocity deviation in the local-level rectangular coordinates can be expressed as

$$\Delta \dot{\mathbf{r}}^* = \begin{bmatrix} \Delta \dot{x}^* \\ \Delta \dot{y}^* \\ \Delta \dot{z}^* \end{bmatrix} = \begin{bmatrix} \Delta \dot{x} + \dot{v} \Delta z \\ \Delta \dot{y} \\ \Delta \dot{z} - \dot{v} \Delta x \end{bmatrix} = \frac{(\mu p)^{1/2}}{r^2} \begin{bmatrix} \Delta x' + \Delta z \\ \Delta y' \\ \Delta z' - \Delta x \end{bmatrix} \quad (4)$$

where primes denote differentiation with respect to true anomaly.

Let the perturbation $\Delta \mathbf{r}$ be transformed

$$\Delta \mathbf{r} = \begin{bmatrix} \Delta x \\ \Delta y \\ \Delta z \end{bmatrix} = r \begin{bmatrix} L_x \\ L_y \\ L_z \end{bmatrix} = r \mathbf{L} \quad (5)$$

where \mathbf{L} is an arbitrary vector.

Substituting Eq. (5) into Eq. (1), converting the time differentiation to true anomaly differentiation using two-body reference values, and taking due cognizance of the two-body

Received April 17, 1964.

† Senior Technical Specialist, Autonetics Division. Member AIAA.

integrals of the reference trajectory, yields the following equations in terms of the component of \mathbf{L} :

$$L_x'' + 2L_x' = 0 \quad (6)$$

$$L_y'' + L_y = 0 \quad (7)$$

$$L_z'' - 2L_z' - 3(r/p) L_z = 0 \quad (8)$$

This set is integrable as shown below. First note that the out-of-plane component L_z is directly integrable:

$$L_y = K_5 cv + K_6 sv \quad (9)$$

The in-plane equations (6) and (8) are coupled and are integrated as follows: from Eqs. (6) and (8) there results

$$L_x' = -2L_x + K_1 \quad (10)$$

$$L_z'' + [4 - 3(r/p)] L_z = 2K_1 \quad (11)$$

An integral to Eq. (11) can be obtained upon substituting $(p/r) = 1 + ecv$ and seeking an integrating factor. It can be shown that $W = sv(1 + ecv)$ is this integrating factor yielding the equation from which the integral L_z is obtained:

$$\frac{d}{dv} \left(W^2 \frac{d}{dv} \left[\frac{L_z}{W} \right] \right) = 2K_1 W$$

$$L_z = 2K_1 W \int_{v_0}^v \frac{1}{W^2} dv \int_{v_0}^v W dv + C_2 W \int_{v_0}^v \frac{1}{W^2} dv + C_3 W \quad (12)$$

formations. These transformations are expressed in terms of eccentric anomaly E for elliptic orbits ($e < 1$) and hyperbolic eccentric anomaly F for hyperbolic orbits ($e > 1$). When re-transformed back to true anomaly, the integrals for both types of orbits are found to be completely equivalent;

$$M_1 = -\frac{3e^2 n^* \tau}{(1-e^2)} + \frac{1}{(1-e^2)sv sv_0} \times \left[2e \left(\frac{r}{p} sv_0 - \frac{r_0}{p} sv \right) + s(v - v_0) \right] \quad (15)$$

$$M_2 = -\frac{1}{2} \frac{p}{r} \left\{ -3 \frac{p}{r} \frac{en^* \tau}{(1-e^2)} + \frac{r r_0}{p p e(1-e^2)} \times \left[\frac{p}{r_0} \left(\frac{p}{r} + 1 \right) esv + \left(\frac{p}{r} \right)^2 \frac{1}{sv_0} \left(-2e + \frac{p}{r_0} cv_0 \right) \right] \right\} \quad (16)$$

Substituting Eqs. (9, 13, and 14) into Eqs. (5) and (4), and regrouping the results, the following matrix equation can be written:

$$\mathbf{x} = \mathbf{Q} \mathbf{K} \quad (17)$$

where

\mathbf{x} = state vector = $\text{col}(\Delta x, \Delta y, \Delta z, \Delta \dot{x}^*, \Delta \dot{y}^*, \Delta \dot{z}^*)$

\mathbf{K} = constant vector = $\text{col}(K_1, K_2, K_3, K_4, K_5, K_6)$

$$\mathbf{Q} = \begin{bmatrix} -\frac{r}{p} \left(1 + \frac{p}{r} \right) sv & \frac{p}{r} & -2 \frac{r}{p} M_2 & \frac{r}{p} & 0 & 0 \\ 0 & 0 & 0 & 0 & \frac{r}{p} cv & \frac{r}{p} sv \\ cv & esv & sv M_1 & 0 & 0 & 0 \\ -n^*(e + cv) & 0 & n^* cv & n^* esv & 0 & 0 \\ 0 & 0 & 0 & 0 & -n^* sv & n^*(e + cv) \\ n^* \frac{p}{r} sv & -n^* \left(\frac{p}{r} \right)^2 & n^* \left(\frac{p}{r} \right)^2 M_3 & -n^* \frac{p}{r} & 0 & 0 \end{bmatrix} \quad (18)$$

$$L_z = \frac{K_1}{e} \frac{p}{r} cv + K_2 \frac{p}{r} sv + K_3 \frac{p}{r} sv \int_{v_0}^v \frac{1}{W^2} dv \quad (13)$$

Substituting Eq. (13) into Eq. (10) and integrating yields

$$L_x = -\frac{K_1}{e} sv \left(1 + \frac{p}{r} \right) + \frac{K_2}{e} \left(\frac{p}{r} \right)^2 - 2K_3 \int_{v_0}^v W dv \int_{v_0}^v \frac{1}{W^2} dv + K_4 \quad (14)$$

The integrals in Eqs. (13) and (14), respectively, denoted by M_1 and M_2 , can be easily evaluated using standard trans-

Transition Matrix

The error coefficients are obtained by converting the solution equation (17) to an initial value problem. This is accomplished as follows: from Eq. (17), at the initial epoch,

$$\mathbf{x}_0 = \mathbf{Q}_0 \mathbf{K} \quad (19)$$

Eliminating the constant vector \mathbf{K} yields

$$\mathbf{x} = \mathbf{Q} \mathbf{Q}_0^{-1} \mathbf{x}_0 \quad (20)$$

where $\mathbf{Q} \mathbf{Q}_0^{-1}$ is the desired result given in Table 1 of Ref. 1. To develop the product analytically, the inverse at the initial epoch is obtained from Eq. (18) by direct inversion,

$$\mathbf{Q}_0^{-1} = \begin{bmatrix} -sv_0 & 0 & \frac{1}{e} \frac{p}{r_0} & \frac{1}{n^*} \frac{r_0}{pe} & 0 & 0 \\ \frac{cv_0}{e} & 0 & \frac{e - (p/r_0) cv_0}{e^2 sv_0} & -\frac{1}{n^* e} \frac{r_0}{p} ctn & 0 & 0 \\ 0 & 0 & \frac{1}{e} \left(\frac{p}{r_0} \right)^2 & \frac{1}{n^* e} \frac{p}{r_0} & 0 & \frac{1}{n^*} sv_0 \\ -\frac{(e + cv_0)}{e} & 0 & \frac{p sv_0}{r_0 e} & \frac{1}{n^* e} \frac{r_0}{p} \left(1 + \frac{p}{r_0} \right) \frac{sv_0}{e} & 0 & -\frac{1}{n^*} \frac{cv_0}{e} \\ 0 & (e + cv_0) & 0 & 0 & -\frac{1}{n^*} \frac{r_0}{p} sv_0 & 0 \\ 0 & sv_0 & 0 & 0 & \frac{1}{n^*} \frac{r_0}{p} cv_0 & 0 \end{bmatrix} \quad (21)$$

Premultiplying Eq. (21) by Eq. (18) will yield the initial value solution to Eqs. (1) and (4), which constitute the transition matrix as given by Table 1 of Ref. 1.

Discussion

Aside from its intrinsic usefulness for navigation-guidance mechanization, it was found that the locally level in-plane, out-of-plane frame of reference was the most convenient for performing the integration primarily because of the decoupling that takes place between in-plane and out-of-plane coordinates. The simplification which this decoupling provides eases immeasurably the analytic manipulations. Needless to say, these manipulations are still quite laborious whether one perturbs the integrals or integrates the perturbations.

The relationship of Eqs. (6-8) to Geyling's equations⁴ should be noted. If Geyling had performed the transformation equation (5), then Eqs. (6-8) would result. Without this transformation, the integral would have been difficult to obtain.

Danby³ also gives a detailed theory for two-body error coefficients. His matrizants are developed as perturbations of two-body integrals with respect to the orbit constants. The transition matrix is obtained upon multiplying two 6×6 matrizants, each evaluated at the respective epoch. It should be noted that the Q and Q_0^{-1} matrices here obtained are, in reality, matrizants with respect to a different set of constants.

References

- ¹ Kochi, K. C., "Exact first-order navigation-guidance mechanization and error propagation equations for two-body reference orbits," AIAA J. 2, 365-368 (1964).
- ² Kochi, K. C., "An introduction to midcourse navigation-guidance," Autonetics Rept. EM 262-265 (October 1962).
- ³ Danby, J. M., "The matrizant of Keplerian motion," AIAA J. 2, 16-19 (1964).
- ⁴ Geyling, F. T., "Coordinate perturbations from Keplerian orbits," AIAA J. 1, 1899-1901 (1963).
- ⁵ Kochi, K. C., "Navigation-guidance mechanization equations for two-body orbits," Autonetics Rept. TM 243-2-150 (May 1963).

Flow Field in a Swirl Chamber

D. H. TSAI*

Institut für Hochtemperaturforschung der Technischen Hochschule Stuttgart, Germany

Introduction

THE operation of a swirl-stabilized plasmajet generator has been described recently by Pfender.¹ Figure 1 shows such a chamber with its typical dimensions. Gas is introduced into the chamber from symmetrically arranged peripheral jets at one (or both) end of the chamber and leaves from the central holes in the end plates. The tangential component of the jets drives the gas in rotation. As a plasmajet generator, the end plates serve as electrodes for discharging an arc along the chamber axis. The gas thus heated by the arc streams out of the central holes and forms

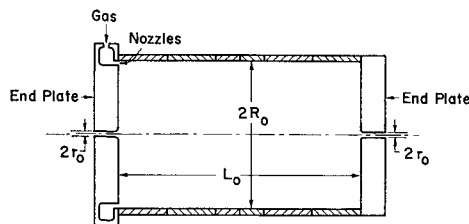


Fig. 1 Schematic diagram of a swirl chamber. In the experimental setup, $D_0 = 2R_0 = 60$ mm, $L_0 = 30$ -100 mm, $2r_0 = 2$ mm. Six nozzles each with exit area of 1 mm^2 , nozzle axes at 10° from swirl chamber end plate.

plasmajets. The arc column inside the chamber is quite stable, but the exact mechanism of the stability is not clear.

The purpose of this note is to describe some quantitatively consistent measurements on the flow field in a series of swirl chambers with different L_0/D_0 ratios. These measurements were made without the arc along the axis. Other experiments, however, have shown that the radial pressure distribution remained qualitatively unaltered in the presence of the arc. A fuller account of this work and a discussion of the influence of the mass flow on the arc column stability will be published elsewhere.

Experiments

The quantities measured were the tangential component of the flow velocity, the flow direction, and the total pressure at different radial and axial positions in the swirl chamber. The tangential velocity components were measured by means of a series of flat-sided propellers (anemometers) mounted on jewel bearings located along the chamber axis. By assuming the gas in the central core to rotate as a solid body and the drag coefficient of the propeller element to remain constant, it was possible to evaluate the rotational speed ω of the gas core from the change of the rotational speed of the propeller ω_p due to a small increase in the propeller diameter. From this information, and with similar assumptions, it was possible to obtain the rotational speed of successively larger cylindrical gas layers as the propeller diameter was successively increased.

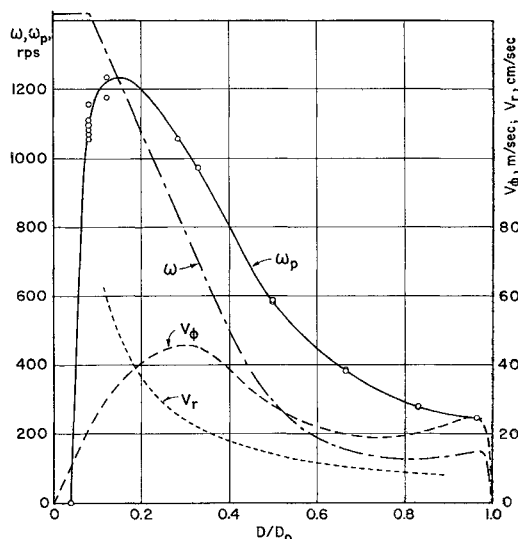


Fig. 2 Typical variation of the measured propeller rotational speed ω_p with propellers of different diameters D . For this series, the propellers were located at $L/L_0 = 0.45$ from the nozzle end, $L_0 = 100$ mm. Upstream nozzle pressure $P_p = 1.0 \text{ kg/cm}^2$. The rotational speed ω and the tangential velocity component V_ϕ of the gas were obtained from the ω_p curve. The radial velocity component V_r was computed from the measured flow rate.

Received May 1, 1964. This investigation was carried out at the Institut für Hochtemperaturforschung, host institution to the author while he was on a training assignment from the National Bureau of Standards. The author gratefully acknowledges his indebtedness to K. H. Höcker and other members of the Institut and to the National Bureau of Standards for making this work possible.

* Now Aeronautical Research Engineer, National Bureau of Standards, Washington, D. C.